Single-photon all-optical switching using waveguide-cavity quantum electrodynamics

Peter Bermel, Alejandro Rodriguez, Steven G. Johnson, John D. Joannopoulos, and Marin Soljačić
Center for Materials Science and Engineering, Massachusetts Institute of Technology, Cambridge, Massachusetts 02139, USA
(Received 7 May 2006; revised manuscript received 26 June 2006; published 24 October 2006)

This paper demonstrates switching of a single signal photon by a single gating photon of a different frequency, via a cross-phase-modulation. This effect is mediated by materials exhibiting electromagnetically induced transparency (EIT), which are embedded in photonic crystals (PhCs). An analytical model based on waveguide-cavity QED is constructed for our system, which consists of a PhC waveguide and a PhC microcavity containing a four-level EIT atom. It is solved exactly and analyzed using experimentally accessible parameters. It is found that the strong coupling regime is required for lossless two-photon quantum entanglement.

DOI: 10.1103/PhysRevA.74.043818 PACS number(s): 42.50.Gy, 42.50.Pq, 42.70.Qs

Several emerging technologies, such as integrated all-optical signal processing and all-optical quantum information processing, require strong and rapid interactions between two distinct optical signals [1]. Achieving this goal is a fundamental challenge because it requires a unique combination of large nonlinearities and low losses. The weak nonlinearities found in conventional media mean that large powers are required for switching. However, nonlinearities up to 12 orders of magnitude larger than those observed in common materials [2] with low losses can be achieved using materials exhibiting electromagnetically induced transparency (EIT) [2–4]. One can then envision inducing strong interactions between two very weak signals of different frequencies by placing a four-level EIT atom in a high-Q cavity, so that a very small signal at a specific atomic transition frequency could shift another resonant frequency of the system by a measurable amount [5]. This approach differs from several optical switching schemes for small numbers of photons that have previously been discussed in the literature. One of the pioneering papers in this area used a single three-level atom with a V-level structure in an optical cavity to induce a cross-phase-modulation of 16° between two photons [6]. EIT offers even further opportunities in terms of larger nonlinearities and greater tunability, which has directed much subsequent work in this direction. EIT materials have been predicted to cause a photon blockade effect, where the state of a cavity can be switched by the self-phase-modulation of a single photon [7–9] or several photons [10,11]. This effect has recently been observed experimentally [12]. Reference [13] predicts that ensembles of EIT atoms can be modulated to create quantum entangled states for a small number of photons. An alternative method is discussed in Ref. [14], whereby a laser beam can control the relative populations of a two-state system embedded in a photonic crystal (PhC), which switches its transmission properties at low power levels.

Reference [5] semiclassically demonstrates the strong interaction of very low intensity fields that can be mediated by EIT materials. This work extends that idea to the quantum regime by writing down the waveguide-cavity QED Hamiltonian for a system consisting of one or a few four-level EIT atoms strongly coupled to a PhC cavity mode, which in turn is coupled to a PhC waveguide, and solving it exactly. Furthermore, an approach to calculating the relevant parameters from first principles is demonstrated. It should be experimentally feasible, with EIT having already been demonstrated in a Pr-doped Y_2SiO_5 crystal [15,16]. Note that compared to EIT systems, such as Na BECs displaying narrow bandwidths (e.g., 2 MHz [2]), switching can occur over much larger bandwidths even for single-photon power levels (e.g., 2 GHz, using the parameters from Ref. [17]) because the PhC cavity compensates for weaker nonlinearities, as demonstrated in this paper. Furthermore, this approach utilizes PhCs, which offer confinement of light to high-quality factor microcavities with low modal volumes, which facilitates strong coupling between light and matter. The emergence of phenomena associated with the quantization of the probe and gate fields (e.g., Rabi-splitting) is discussed. Finally, it is shown that switching behavior can be achieved with single probe and gate photons, and the physical parameters needed to achieve such operations are calculated.

Consider the following design, illustrated in Fig. 1. There is a cavity that supports two resonant modes, one with a resonant frequency ω_{res} and the other with a control frequency ω_{con}, enclosing a single four-level EIT atom with coupling strengths g_{ij} and atomic transition frequencies ω_{ij}, where i and j refer to the initial and final atomic states, respectively. The EIT dark state is created by adding a classical coupling field to the cavity with frequency ω_{23} and Rabi frequency $2\Omega_c$; all other quantities are treated quantum me-

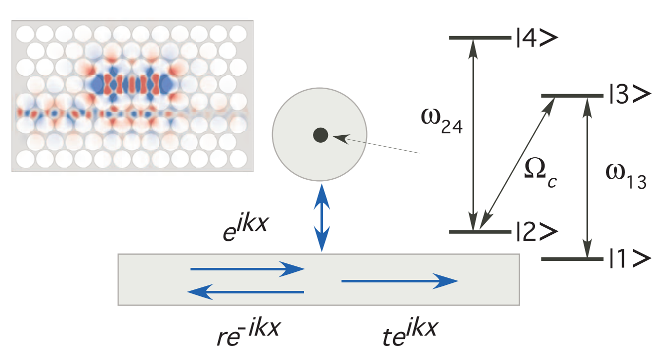

FIG. 1. (Color) Schematic illustration of the system investigated. A waveguide is coupled to a cavity with an EIT atom at its center. In the upper left-hand corner, an FDTD simulation that can be used to calculate the model parameters is shown.

chanically. In general, any number of coupling schemes between the cavity and one or more waveguides could be utilized. However, in this paper, the $\omega_{\rm res}$ cavity mode is side coupled to an adjacent single-mode waveguide with a radiative linewidth $\Gamma_w=\omega_{\rm res}/2Q_w=V_w^2/v_g$, where Q_w is the quality factor of the $\omega_{\rm res}$ cavity mode, V_w is the coupling strength, and v_g is the group velocity in the waveguide—its dispersion relation $\omega(k)$ is assumed to be approximately linear near the $\omega_{\rm res}$ resonance. For relatively strong cavity-waveguide couplings, radiative couplings out of the system are much smaller and may be neglected. Also, the $\omega_{\rm con}$ resonance is designed to have a much smaller decay rate $\Gamma_{\rm con}=\omega_{\rm con}/2Q_{\rm con}$. This can be achieved by starting with two dipole modes, one with an even symmetry coupled strongly to the waveguide and one with an odd symmetry exactly decoupled from the waveguide. A slight shift in the cavity position can then create a slight coupling that, nonetheless, creates a substantial disparity in quality factors, i.e., $Q_{\rm con}\gg Q_w$ (see, e.g., Refs. [18,19]). Alternatively, one could use two cavities to create even and odd modes with substantially different quality factors [20]. In the absence of an atom, this design produces a Lorentzian line shape for the *reflection* (because of the side coupling), centered around $\omega_{\rm res}$ [21]. A PhC implementation of this is shown in the upper left-hand corner of Fig. 1—a triangular lattice of air holes in silicon with radius $0.48a$ that has a complete 2D photonic bandgap. A similar geometry has been used for quantum dots in PhC microcavities, as in Ref. [17]. That experimental system exhibits a critical photon number $m_0=\Gamma_3^2/2g^2=0.55$ and critical atom number $N_0=2\Gamma_w\Gamma_3/g^2=4.2$. Ideally, both of these numbers would be <1 for quantum information processing [22]. It should be possible to achieve this goal with improvements in Q or modal volume $V_{\rm mode}$, or by placing several atomic or quantum dot systems in the same microcavity. Note that it could also be possible to achieve similar behavior with other physical systems, such as high-finesse Fabry-Perot optical microcavities [23], or ultrahigh-Q toroidal microresonators [24].

Combining Ref. [8]'s Hamiltonian for an EIT atom in a cavity and Ref. [25]'s Hamiltonian for a waveguide interacting with a cavity yields

$$\begin{aligned}H/\hbar &= \sum_k \omega_k a_k^\dagger a_k + \omega_{\rm res}a^\dagger a + \omega_{\rm con}b^\dagger b + \sum_k V_w(a_k^\dagger + a_k)(a^\dagger \\ &\quad + a) + \omega_{21}\sigma_{22} + (\omega_{13} - i\Gamma_3)\sigma_{33} + (\omega_{14} - i\Gamma_4)\sigma_{44} \\ &\quad + \Omega_c(\sigma_{32}+\sigma_{23})\cos(\omega_{23}t) + g_{13}(a^\dagger\sigma_{13} + a\sigma_{31}) \\ &\quad + g_{24}(b^\dagger\sigma_{24} + b\sigma_{42}) \qquad (1)\end{aligned}$$

where a_k are the annihilation operators for waveguide states of wave vector k and frequency ω_k; a and b are the annihilation operators for cavity photon states of frequencies $\omega_{\rm res}$ and $\omega_{\rm con}$, respectively (which are considered in this paper to be unoccupied or singly occupied); σ_{ij} are the projection operators that take the atomic state from j to i; Γ_3 is the nonradiative decay rate of the third level; Γ_4 is the nonradiative decay rate of the fourth level; $\Delta\tilde{\omega}_{13}=\omega_{13}-\omega_{\rm res}-i\Gamma_3$ is the complex detuning of the $1\rightarrow 3$ transition from $\omega_{\rm res}$; and $\Delta\tilde{\omega}_{24}=\omega_{24}-\omega_{\rm con}-i\Gamma_4$ is the complex detuning of the $2\rightarrow 4$ transition from $\omega_{\rm con}$. In this paper, the cavity resonance is designed to match the $1\rightarrow 3$ transition, i.e., $\omega_{\rm res}=\omega_{13}$, so that $\Delta\tilde{\omega}_{13}=i\Gamma_3$. Also, although $\Delta\tilde{\omega}_{24}$ is predominantly real, in general, there is an imaginary part corresponding to absorption losses in the fourth level. However, when the detuning greatly exceeds the decay rate of the upper level, this contribution may be neglected. Losses from the second atomic level are also neglected, since, typically, it is a metastable state close to the first atomic level in energy. Finally, although, in general, the two cavity modes will have at least slightly different frequencies, we set $\omega_{\rm con}=\omega_{\rm res}$ for simplicity.

The Hamiltonian in Eq. (1) can then be rewritten in real space and separated into a diagonal part

$$\begin{aligned}H_o/\hbar &= \omega_{\rm res}\int dx[a_R^\dagger(x)a_R(x) + a_L^\dagger(x)a_L(x)] + \omega_{\rm res}(a^\dagger a + b^\dagger b \\ &\quad + \sigma_{33} + \sigma_{44}) + \omega_{21}(\sigma_{22}+\sigma_{44}), \qquad (2)\end{aligned}$$

where a_L and a_R refer to left and right moving waveguide photons, respectively, as well as an interaction part

$$\begin{aligned}H_I/\hbar &= \int dx\{a_R^\dagger(x)(-iv_g\partial_x - \omega_{\rm res})a_R(x) + a_L^\dagger(x)(iv_g\partial_x \\ &\quad - \omega_{\rm res})a_L(x) + V_w\delta(x)[a_R^\dagger(x)a + a_R(x)a^\dagger + a_L^\dagger(x)a \\ &\quad + a_L(x)a^\dagger]\} + \Omega_c(\sigma_{23}+\sigma_{32}) + g_{13}(a^\dagger\sigma_{13} + a\sigma_{31}) \\ &\quad - i\Gamma_3\sigma_{33} + \Delta\tilde{\omega}_{24}\sigma_{44} + g_{24}(b\sigma_{42} + b^\dagger\sigma_{24}) \qquad (3)\end{aligned}$$

via the interaction picture (using the rotating-wave approximation [26]), where the total system Hamiltonian is given by $H=H_o+H_I$. The eigenstate for the system can be written as

$$\begin{aligned}|\psi_k\rangle &= \Big\{\int dx[\phi_{k,R}^+(x)a_R^\dagger(x) + \phi_{k,L}^+(x)a_L^\dagger(x)] + e_k a^\dagger + f_k\sigma_{31} \\ &\quad + h_k\sigma_{21} + p_k\sigma_{41}b\Big\}|0,0,1\rangle_{\rm phc}\otimes|1\rangle_{\rm atom} \qquad (4)\end{aligned}$$

where

$$\phi_{k,R}^+(x) = e^{ikx}[\theta(-x) + t\theta(x)] \qquad (5)$$

$$\phi_{k,L}^+(x) = re^{-ikx}\theta(-x),$$

e_k is the probability amplitude of the cavity photon at $\omega_{\rm res}$, and f_k, h_k, and p_k are the occupations of the third, second, and fourth atomic levels, respectively. t and r are the waveguide transmission and reflection amplitudes, respectively. All of these parameters are determined when the eigenequation is solved below. $|0,0,1\rangle_{\rm phc}\otimes|1\rangle_{\rm atom}$ is an eigenstate consisting of a direct product of a photonic state (phc) and an atomic state (atom). The photonic state consists of zero photons in the waveguide, zero photons in the cavity at $\omega_{\rm res}$, and one photon in the cavity at $\omega_{\rm con}$, respectively. The atomic state consists of a single atom in its ground state. Note that $|\psi_k\rangle$ is written in terms of an annihilation operator b in order to simplify the notation, which would otherwise require $b^\dagger$ operators in all but one term.

Applying the Hamiltonian [Eq. (3)] to the time-independent eigenvalue equation $H_I|\psi_k\rangle=\hbar\epsilon_k|\psi_k\rangle$, where

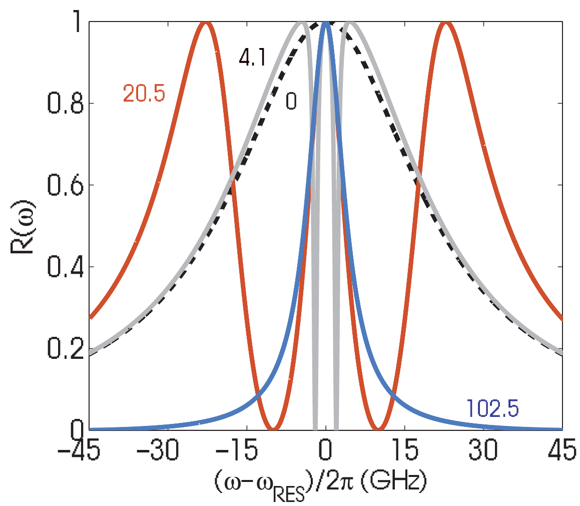

FIG. 2. (Color) Waveguide reflection for a lossless three-level EIT atom for the four labeled values of the atomic coupling strength g_{13} (in gigahertz). The radiation rate $\Gamma_w=21.5$ GHz and the ratio $g_{13}/\Omega_c=2$ are fixed. Larger g_{13} produces larger peak separations (the blue curve shows Rabi peaks outside of the plot), favorable for switching.

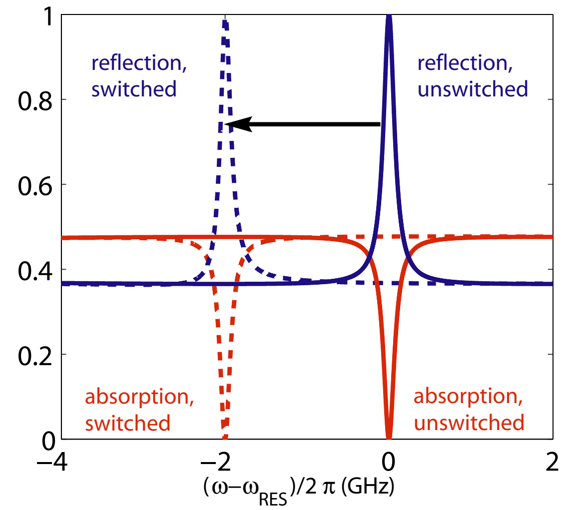

FIG. 3. (Color) Waveguide reflection (blue) and absorption (red) in the absence (solid) and presence (dashed) of an control photon, demonstrating nonlinear single-photon switching ($\Gamma_w=21.5$ GHz, $g_{13}=20.5$ GHz, $\Omega_c=2$ GHz, $\Gamma_3=30$ GHz, $g_{24}=8$ GHz, and $\Delta\tilde{\omega}_{24}=30$ GHz).

$\epsilon_k=\omega-\omega_{\rm res}$, and solving for the reflection coefficient yields $|r(\epsilon_k)|^2=|\Gamma_w/(\xi-i\Gamma_w)|^2$, where

$$\xi=\epsilon_k-\frac{g_{13}^2}{\epsilon_k+i\Gamma_3-\frac{\Omega_c^2}{\epsilon_k-g_{24}^2/(\epsilon_k-\Delta\tilde{\omega}_{24})}} \qquad (6)$$

The parameters g_{13}, V_w (or Γ_w), v_g, and Ω_c of Eq. (3) can be determined from a numerical solution to Maxwell's equations (as in Ref. [27]) as follows. First, the cavity mode is excited by a source, and the modal volume of the cavity is found from the field patterns by $V_{\rm mode}=(\int_{\rm mode} d^3x\,\epsilon|\mathbf{E}|^2)/\epsilon|\mathbf{E}_{\rm max}|^2$. One can then apply the formula $g_{13}=\sqrt{\pi e^2 f_{13}/m\epsilon V_{\rm mode}}$ [28], where e is the elementary electric charge, ϵ is the dielectric constant of the medium in which the atomic system is embedded, m is the free electron mass, and f_{13} is the oscillator strength for the $|1\rangle\to|3\rangle$ transition (1/2 in Na[2]). The linewidth Γ_w can be calculated by examining the decay rate of the field in the cavity mode. The waveguide group velocity is given by $v_g=[d\omega(k)/dk]|_{\omega=\omega_{\rm res}}$. Finally, the Rabi frequency Ω_c can be estimated from quantum mechanics by first determining the vacuum Rabi splitting for the $2\to3$ atomic transition g_{23}, and then multiplying by $\sqrt{n}$, where n is the number of ω_{23} photons.

First, consider the case of a two-level atomic system (i.e., $\Omega_c=0$, $g_{24}=0$), with a waveguide coupling Γ_w and a nonradiative decay rate Γ_3. For a fixed atom-photon coupling g_{13} and zero nonradiative absorption, the single resonant mode at $\epsilon_k=0$ experiences a Rabi splitting into two orthogonal linear superpositions of the cavity and atom modes at $\epsilon_k=\pm g_{13}$. As long as one remains in the strong coupling regime $g_{13}>|\Gamma_3-\Gamma_w|/2$, the absorption for all frequencies increases nearly linearly with Γ_3 for small Γ_3 [29].

However, in the opposite regime of weak coupling ($g_{13}<|\Gamma_3-\Gamma_w|/2$), the normal modes of the system are mostly photonic (lossless) or mostly atomic (very lossy). This phenomenon eliminates the Rabi splitting and gives rise to a reflection nearly indistinguishable from a system without an atom for sufficiently large Γ_3.

Now, consider a three-level atomic system without losses in the strong coupling regime. Compared to the two-level system, a third mode, corresponding to the dark state of the EIT atom, will emerge at $\epsilon_k=0$ between the previously observed Rabi-split peaks. The dark eigenstate is given by $|\psi\rangle_{\rm dark}=[a^\dagger-(g_{13}/\Omega_c)\sigma_{21}]|0,0,0\rangle_{\rm phc}\otimes|1\rangle_{\rm atom}$. The width of the central peak is expected to scale as $(\Omega_c/g_{13})^2$ for small Ω_c/g_{13} [13]. If one substitutes the expression given in Ref. [28] for g_{13}, one obtains the classical results found in Refs. [2,5]. Meanwhile, the width of the side peaks is set by Γ_w and remains roughly constant as one tunes the parameters of the system.

In Fig. 2, $g_{13}/\Omega_c=2$ while g_{13} is varied. It is shown that as g_{13} is decreased, the central resonance width stays constant, while the distance between the central and Rabi-split peaks becomes smaller. For use in applications, it therefore seems optimal to have a large Rabi splitting, corresponding to the very strong coupling limit, which can also be viewed as corresponding to critical photon and atom numbers much less than 1. The experimental values for a system with a single quantum dot emitting a single photon observed in Ref. [17] correspond to a regime where $g_{13}\approx\Gamma_w$ — specifically, they find that for operation at $\lambda=1.182$ μm, $g_{13}=20.5$ GHz and $\Gamma_w=21.5$ GHz; note that PhC microcavities are optimal for simultaneously decreasing Γ_w and increasing g_{13}.

Now, consider a four-level system with a control photon present. Two possible effects can be induced by the control photon. When the control frequency $\omega_{\rm con}$ is close to the electronic transition frequency ω_{24}, an Autler-Townes doublet is observed; upon detuning, an AC-Stark shift will be induced in this system instead [5,8]. The latter effect has been suggested as a switching mechanism in Refs. [5,30,31]. This can

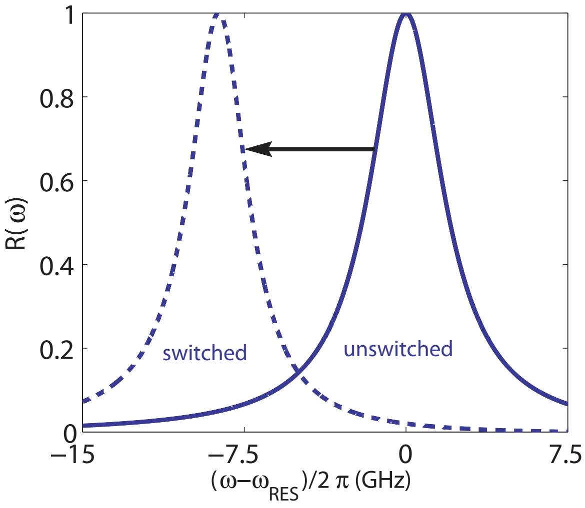

FIG. 4. (Color) Waveguide reflection with (dashed) and without (solid) a control photon, demonstrating lossless switching, where a higher quality factor has made the resonant peaks narrow enough to be shifted by more than their full width at half maximum by a single photon (Γ_w=3 GHz, g_{13}=20.5 GHz, Ω_c=30 GHz, Γ_3=0 GHz, g_{24}=30 GHz, and $\Delta\tilde{\omega}_{24}$=20 GHz).

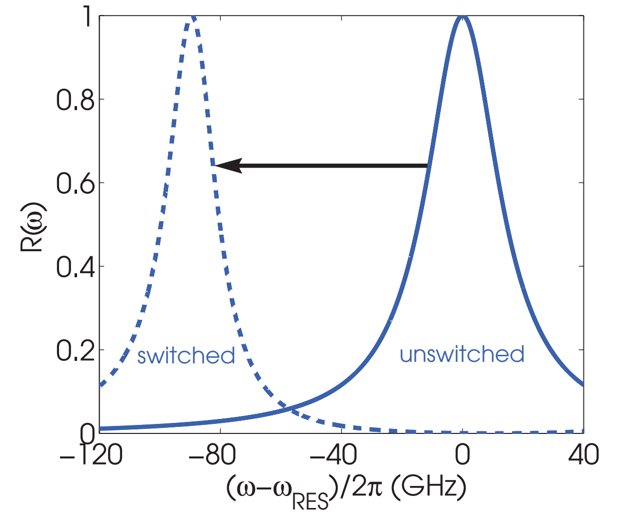

FIG. 5. (Color) Waveguide reflection with (dashed) and without (solid) a control photon, demonstrating lossless switching, where multiple (49) EIT atoms have been used to push the Rabi-split peaks farther away in the presence of negligible loss (Γ_w=21.5 GHz, g_{13}=143.5 GHz, Ω_c=210 GHz, Γ_3=0 GHz, g_{24}=210 GHz and $\Delta\tilde{\omega}_{24}$=20 GHz).

be shown by using Eq. (6) to calculate the poles of the EIT term in the reflection, i.e., set $\epsilon_k - g_{24}^2/(\epsilon_k - \Delta\tilde{\omega}_{24})=0$, which yields $\epsilon_k = \pm g_{24}$ for no detuning, and $\epsilon_k \approx -g_{24}^2/\Delta\tilde{\omega}_{24}$ for a large detuning, matching the semiclassical result found in Ref. [5].

Single-photon switching is obtained when the reflection peak is shifted by an amount greater than its width, via the presence or absence of one control photon. In order to achieve this goal, one can take two different approaches. First, in the regime where $g_{13} \approx \Gamma_w$, as in Ref. [17], one can introduce an absorption via $\Gamma_3 \neq 0$, and thus absorb the majority of light not coupled to the dark state. In Fig. 3, the reflection and absorption are plotted for an optimized value of Γ_3=30 GHz, both before and after switching. As shown, reflections at the Rabi-split frequencies are decreased substantially (to ~40%), while full reflection is still observed at the central, EIT-narrowed peak. Furthermore, in the presence of a single detuned control photon, it is possible to switch the peak reflection frequency by an amount greater than the EIT-narrowed central peak width. A second, lossless approach, appropriate if producing a large nonradiative decay Γ_3 or small Ω_c is difficult in a single-atom device, is to enhance the ratio g_{13}/Γ_w. This goal can be achieved by either decreasing Γ_w or V_{mode}, or by increasing the number of atoms from one to N. The first example of switching by decreasing the waveguide coupling is shown in Fig. 4, where the waveguide coupling width Γ_w is decreased by about a factor of 7 to Γ_w=3 GHz. Now the peaks are narrow enough that a single photon of frequency ω_{con} can shift the peak by more than the full width at half maximum. The second example of switching, by increasing the number of atoms is illustrated in Fig. 5. In general, it is clear that increasing the number of atoms collectively oscillating will improve the coupling strength; in the special case where each atom has equal coupling to the field, the N-atom treatment in Ref. [32] shows that the coupling constant $g_{13} \rightarrow g'_{13} = g_{13}\sqrt{N}$. Furthermore, one can generalize the arguments of Ref. [32] to a four-level system of N atoms to show that the other coupling constants g_{24} and Ω_c will scale in an identical fashion (i.e., $g_{24} \rightarrow g'_{24} = g_{24}\sqrt{N}$, $\Omega_c \rightarrow \Omega'_c = \Omega_c\sqrt{N}$). This collective Rabi oscillation separates the Rabi-split peaks much further from the central peak. Figure 5 shows switching exploiting this phenomenon based on parameters from Ref. [17] and using N=49. The advantage of this lossless switching scheme is that one obtains a substantially greater tuning range and contrast (the difference between the peaks and the troughs) than with the lossy ($\Gamma_3 \neq 0$) scheme.

In conclusion, the reflection peak of a waveguide-cavity system can be switched in and out of resonance by a single gating photon, assuming realistic experimental parameters. Thus, one photon can be used to gate another photon of a different frequency, via a Kerr cross-phase-modulation. This approach is distinct from the photon blockade system where self-phase-modulation is responsible for the switching behavior. Under proper circumstances, this can give rise to two-photon entangled states. The integration of microcavities and waveguides in the same photonic crystal means that the entanglement could be preserved, in principle, throughout the system, which could be of use for quantum information processing [22].

We thank Y. Chong, L. V. Hau, A. Karalis, M. Ibanescu, and J. Shapiro for useful discussions. One of the authors (A.R.) was supported by the Department of Energy. This work was supported in part by the MRSEC Program of the NSF under Grant No. DMR 02-13282, and the Army Research Office through the Institute for Soldier Nanotechnologies under Contract No. DAAD-19-02-D0002.

[1] H. Gibbs, *Optical Bistability: Controlling Light with Light* (Academic, New York, 1985).

[2] L. V. Hau, S. E. Harris, Z. Dutton, and C. Behroozi, Nature (London) **397**, 594 (1999).

[3] K.-J. Boller, A. Imamoglu, and S. E. Harris, Phys. Rev. Lett. **66**, 2593 (1991).

[4] E. Arimondo, in *Progress in Optics* (North-Holland, Amsterdam, 1997), Vol. 35, p. 259.

[5] M. Soljacic, E. Lidorikis, J. D. Joannopoulos, and L. V. Hau, Appl. Phys. Lett. **86**, 171101 (2005).

[6] Q. A. Turchette, C. J. Hood, W. Lange, H. Mabuchi, and H. J. Kimble, Phys. Rev. Lett. **75**, 4710 (1995).

[7] A. Imamoglu, H. Schmidt, G. Woods, and M. Deutsch, Phys. Rev. Lett. **79**, 1467 (1997).

[8] M. J. Werner and A. Imamoglu, Phys. Rev. A **61**, 011801(R) (1999).

[9] S. Rebic, S. Tan, A. Parkins, and D. Walls, J. Opt. B: Quantum Semiclassical Opt. **1**, 490 (1999).

[10] K. M. Gheri, W. Alge, and P. Grangier, Phys. Rev. A **60**, R2673 (1999).

[11] A. D. Greentree, J. A. Vaccaro, S. R. de Echaniz, A. V. Durrant, and J. P. Marangos, J. Opt. B: Quantum Semiclassical Opt. **2**, 252 (2000).

[12] K. Birnbaum, A. Boca, R. Miller, A. Boozer, T. Northup, and H. J. Kimble, Nature (London) **436**, 87 (2005).

[13] R. Beausoleil, W. Munro, and T. Spiller, J. Mod. Opt. **51**, 1559 (2004).

[14] S. John, J. Opt. A, Pure Appl. Opt. **3**, S103 (2001).

[15] A. V. Turukhin, V. S. Sudarshanam, M. S. Shahriar, J. A. Musser, B. S. Ham, and P. R. Hemmer, Phys. Rev. Lett. **88**, 023602 (2002).

[16] B. Ham, P. Hemmer, and M. Shahriar, Opt. Commun. **144**, 227 (1997).

[17] T. Yoshie, A. Scherer, J. Hendrickson, G. Khitrova, H. Gibbs, G. Rupper, C. Ell, O. Shchekin, and D. Deppe, Nature (London) **432**, 200 (2004).

[18] S. G. Johnson and J. D. Joannopoulos, *Photonic Crystals: The Road from Theory to Practice* (Kluwer Academic, Dordrecht, 2002).

[19] J. Joannopoulos, R. Meade, and J. Winn, *Photonic Crystals: Molding the Flow of Light* (Princeton University Press, Princeton, NJ, 1995).

[20] W. Suh, Z. Wang, and S. Fan, IEEE J. Quantum Electron. **40**, 1511 (2004).

[21] H. Haus and Y. Lai, J. Lightwave Technol. **9**, 754 (1991).

[22] H. Mabuchi, M. Armen, B. Lev, M. Loncar, J. Vuckovic, H. J. Kimble, J. Preskill, M. Roukes, and A. Scherer, Quantum Inf. Comput. **1**, 7 (2001).

[23] C. Hood, T. Lynn, A. Doherty, A. Parkins, and H. J. Kimble, Science **287**, 1447 (2000).

[24] S. M. Spillane, T. J. Kippenberg, K. J. Vahala, K. W. Goh, E. Wilcut, and H. J. Kimble, Phys. Rev. A **71**, 013817 (2005).

[25] J.-T. Shen and S. Fan, Phys. Rev. Lett. **95**, 213001 (2005).

[26] M. O. Scully and M. S. Zubairy, *Quantum Optics* (Cambridge University Press, Cambridge, England, 1997).

[27] A. Taflove and S. C. Hagness, *Computational Electrodynamics*, 2nd ed. (Artech House, Norwood, MA, 2000).

[28] L. C. Andreani, G. Panzarini, and J.-M. Gerard, Phys. Rev. B, **60**, 13276 (1999).

[29] V. Savona, L. C. Andaani, P. Schwendimann, and A. Quattropani, Solid State Commun. **93**, 733 (1995).

[30] H. Schmidt and A. Imamoglu, Opt. Lett. **21**, 1936 (1996).

[31] S. E. Harris and L. V. Hau, Phys. Rev. Lett. **82**, 4611 (1999).

[32] Y. Yamamoto and A. Imamoglu, *Mesoscopic Quantum Optics* (Wiley, New York, 1999).